



# Interaction of the Mechanosensitive Channel, MscS, with the Membrane Bilayer through Lipid Intercalation into Grooves and Pockets

Tim Rasmussen<sup>1</sup>, Akiko Rasmussen<sup>1</sup>, Limin Yang<sup>2</sup>, Corinna Kaul<sup>3</sup>, Susan Black<sup>1</sup>, Heloisa Galbiati<sup>1</sup>, Stuart J. Conway<sup>3</sup>, Samantha Miller<sup>1</sup>, Paul Blount<sup>2</sup> and Ian Rylance Booth<sup>1</sup>

**1** - School of Medicine, Medical Sciences and Nutrition, University of Aberdeen, Foresterhill, Aberdeen, AB25 2ZD, UK

**2** - Department of Physiology, U.T. Southwestern Medical Center, 6001 Forest Park Road, Dallas, TX 75390-9040, USA

**3** - Department of Chemistry, Chemistry Research Laboratory, University of Oxford, Mansfield Road, Oxford, OX1 3TA, UK

**Correspondence to Samantha Miller, Paul Blount and Ian Rylance Booth:** [tim.rasmussen@uni-wuerzburg.de](mailto:tim.rasmussen@uni-wuerzburg.de), [Limin.Yang@utsouthwestern.edu](mailto:Limin.Yang@utsouthwestern.edu), [stuart.conway@chem.ox.ac.uk](mailto:stuart.conway@chem.ox.ac.uk), [sam.miller@abdn.ac.uk](mailto:sam.miller@abdn.ac.uk), [Paul.Blount@utsouthwestern.edu](mailto:Paul.Blount@utsouthwestern.edu), [i.r.booth@abdn.ac.uk](mailto:i.r.booth@abdn.ac.uk)

<https://doi.org/10.1016/j.jmb.2019.05.043>

Edited by Nieng Yan

## Abstract

All membrane proteins have dynamic and intimate relationships with the lipids of the bilayer that may determine their activity. Mechanosensitive channels sense tension through their interaction with the lipids of the membrane. We have proposed a mechanism for the bacterial channel of small conductance, MscS, that envisages variable occupancy of pockets in the channel by lipid chains. Here, we analyze protein–lipid interactions for MscS by quenching of tryptophan fluorescence with brominated lipids. By this strategy, we define the limits of the bilayer for TM1, which is the most lipid exposed helix of this protein. In addition, we show that residues deep in the pockets, created by the oligomeric assembly, interact with lipid chains. On the cytoplasmic side, lipids penetrate as far as the pore-lining helices and lipid molecules can align along TM3b perpendicular to lipids in the bilayer. Cardiolipin, free fatty acids, and branched lipids can access the pockets where the latter have a distinct effect on function. Cholesterol is excluded from the pockets. We demonstrate that introduction of hydrophilic residues into TM3b severely impairs channel function and that even “conservative” hydrophobic substitutions can modulate the stability of the open pore. The data provide important insights into the interactions between phospholipids and MscS and are discussed in the light of recent developments in the study of Piezo1 and TrpV4.

© 2019 The Authors. Published by Elsevier Ltd. This is an open access article under the CC BY license (<http://creativecommons.org/licenses/by/4.0/>).

## Introduction

Lipid interactions with membrane proteins are complex and have often proved challenging to measure [1–5]. Despite this, much has been achieved to generate an understanding of the dynamics of proteins–lipid interactions [3,6–13]. All membrane proteins and protein complexes are surrounded by a boundary lipid layer that is in dynamic exchange with bulk lipid [2]. The number of phospholipid (PL) molecules surrounding a protein complex is dictated both by its effective circumference and by the packing of the lipids, which provides a barrier to ions [2,14]. The lipid chains exist in a “fluid” state in the interior

of the bilayer. In a time-averaged manner, the lipid chains will pack closely against the protein surface, following the contours and thereby filling any interstices that exist [9]. In some classes of membrane proteins, for example, some secondary transporters, lipid–protein interactions are a major determinant of conformation [3,13]. It is recognized that lipids are central to the mechanism of gating of mechanosensitive channels (the “force-from-lipids” concept [15–17]).

Modulations of tension in the lipid bilayer, in response to changes in transmembrane turgor, are believed to gate mechanosensitive channels leading to ion (and solute) movement across the membrane

[18–20]. In bacteria, such channels are central to maintaining cellular integrity during severe osmotic transitions that generate extremely high transmembrane turgor pressure [21–23]. High turgor pressure leads to tears in the peptidoglycan layer through which cytoplasm is extruded during cell bursting. The potential damage is countered by the release of solutes through the channel pore. It is implicit in this model that high turgor generates transitions in the bilayer tension [22–26]. An additional factor is that a number of lipid-like molecules can activate mechanosensitive channels in the absence of changes in cell turgor. These molecules include local anesthetics, *lyso*-phospholipids, and polyunsaturated lipids [27–30]. We have only a limited understanding of the molecular mechanism by which tension is sensed and the signal transduced [31,32].

The structures of the bacterial mechanosensitive channels provide both the context for models of tension-sensing via lipid interactions but also clues to the possible mechanism [31–33]. Multiple crystal structures exist for the MscS channel [32,34,35]. The core structure is a heptamer of identical subunits (Figs. 1a and S1a) that oligomerize to form the transmembrane pore and a large cytoplasmic domain. Each subunit contributes three helices to the membrane domain: TM1 and TM2 form antiparallel transmembrane helices that have the potential to interact with the lipids of the bilayer, whereas TM3 is in two parts—seven identical TM3a helices combine to create the transmembrane pore, whereas TM3b lies parallel to the membrane surface and integrates with the upper  $\beta$  sub-domain of the cytoplasmic domain (Fig. 1b). The *Escherichia coli* MscS protein has been solved in two principal states: a closed state in which the pore is sealed by two rings of leucine residues (L105 and L109), brought into proximity by the tight packing of the TM3a helices [34], and an open state in which the TM3a helices have straightened relative to the pore axis and moved apart to break the seal [35]. Concurrent with these changes in organization, the TM1–2 helix pair rotate around the axis of the pore and the TM1–2 helices are packed more closely against the pore helices [35]. Although the static nature of crystal structures has caused them to be treated with caution [19], they frame the argument for the interaction with lipids, which must change during the transition from closed to open [35].

The OPM (Orientations of Proteins in Membranes) database [36] predicts the lipid packing, for a simple planar bilayer, around membrane proteins for which a crystal structure is known. When applied to the closed structure (Fig. 1a, PDB: 2OAU) a clear prediction is made that the cytoplasmic ends of the transmembrane helices (TM1 and TM2) are exposed to the aqueous phase. However, for MscS the lipid-exposed surface is rendered more complex by the presence of pockets created by the TM2, TM3a, TM3b, and

residues in the  $\beta$  subdomain that penetrate the interstices between TM3b helices from adjacent subunits (Fig. 1b) [32]. We have recently proposed that displacement of lipids from the pockets, as a result of increased bilayer tension, favors the open conformation of the channel [32], which is predicted to have smaller pockets.

There are a number of structural features of MscS that lend themselves to this model. First, the overall character of the amino acid residues of TM1–2 and TM3a is hydrophobic [34]. Second, the TM3b helix is amphipathic with the hydrophobic surface predicted to interact with lipids [34] (Fig. S2). Third, hydrophobic residues from the  $\beta$  domain penetrate between the interstices between the seven TM3b helices. The overall effect is of a hydrophobic protein disc (TM3b plus “ $\beta$  domain” side chains) that is perforated at its center by the MscS pore. Thus, the overall character of the residues in this disc, and those exposed from TM3a and TM1–2, creates a hydrophobic pocket that is ideal for lipid occupancy (Fig. 1c). We sought to test the hypothesis that lipids penetrate the pocket and that the hydrophobic character of TM3b is essential to gating of MscS. We have utilized a combination of quenching of introduced Trp residues by brominated lipids [4,5,37,38] and site-directed mutagenesis of the TM3b hydrophobic surface. The data point to deep penetration of the structure of the MscS channel complex by membrane lipids and fatty acids. Furthermore, we show that branched chain lipids cause unique modifications of MscS behavior in liposomes. Finally, we have identified a critical requirement for hydrophobic residues in TM3b, and a specific role for Val122, in determining the tension-sensitivity and the stability of the open state of MscS.

## Results

### Protein–lipid interactions—experimental strategy

Protein lipid interactions are frequently difficult to investigate. However, significant advances have been made by the use of either spin-labeled lipids or brominated lipids [4,5,8,39,40]. For the latter, the bulky bromine atoms cause the fatty acid chains to behave similarly to unsaturated lipids [38]. The quenching of Trp residues by the bromine atoms can give information on accessibility of the residue to lipids and hence create structural insights from the reconstituted membrane protein. Bromine atoms that are distant to the lipid headgroup can “explore” a larger volume of space in a time-dependent manner due to the intrinsic flexibility of the lipid chain. The region close to the headgroup has been suggested to have more limited flexibility compared with the terminal methyl group [41]. Bromine atoms quench Trp residues that are either native or have been introduced by site-directed mutagenesis.

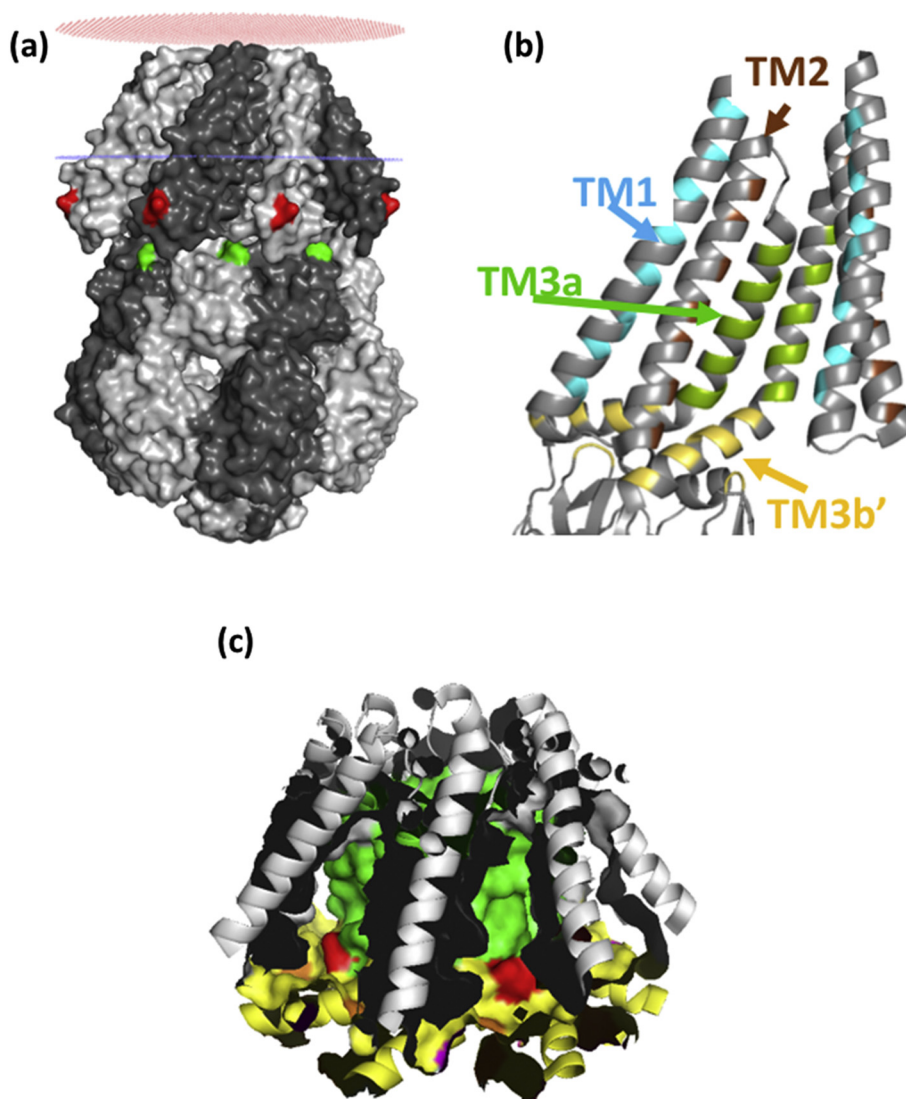


**Fig. 1.** (a) OPM model of surface-rendered closed structure MscS. I57 (red) and I150 (green) are marked. Red and blue rings indicate the position of the lipid/headgroup region of the periplasmic and cytoplasmic leaflets of the bilayer, respectively. (b) Hydrophobic pocket in MscS; seven identical hydrophobic pockets are created by residues on TM1 (cyan), TM2 (brown), TM3a (green), and TM3b'/beta domain (Yellow). The pocket is a volume that is contiguous with the membrane bilayer and is not a binding site for lipids. It is proposed that the lipid chains of the phospholipids that surround the periphery of MscS reversibly and dynamically penetrate the pockets. Only two subunits are shown for clarity. (c) The surface of the pockets are shown with the same color scheme as in panel b. L111 is marked in red. All images are based on the closed structure (PDB: 2OAU).

Quenching has been reported to involve very close proximity between the bromine atoms and the Trp side chain ( $\sim 9$  Å; [42]). Thus, we sought to investigate the protein–lipid interactions in MscS using commercially available and synthetic lipids in combination with site-directed mutagenesis to create mutant proteins at informative positions.

#### Membrane bilayer alignment to TM1

The OPM model [36] of MscS positioning in a planar bilayer (Fig. 1a) suggests that the hydrophobic leaflet

extends approximately from residue N20 to the basic amino acid R46 of TM1 (based on the most complete MscS crystal structure, 5aji.pdb). Previously, it was assumed that the whole paddle, extending to R59, is immersed into the membrane [34], but it is a clear prediction from the OPM model that this region may reside in or below the headgroup region. To investigate the lipid interactions with MscS TM1, potentially lipid-facing residues extending from A21 to I57 were mutated to Trp (SI text; Fig. S3–4). All of the Trp mutants exhibited blue-shifted emission maxima with the exception of

I57W (Table S1), consistent with locations in hydrophobic environments. Raw data for all the Trp mutants analyzed are given in the SI (Table S1). Reconstitution of purified MscS Trp mutant channels was performed into brominated phosphatidyl choline (C-18 BrPC) vesicles, with DOPC as the control (Fig. S5) [32]. To complement these data with more detailed insights, we utilized commercially available C-18 brominated lipids in which the bromine atoms are at different distances from the headgroup (6.7BrPC, 9.10BrPC, and 11.12BrPC). Tryptophan at positions corresponding to residue 21 to residue 51 exhibited high levels of quenching (Fig. 2; Table S1). All of the Trp residues exhibited quenching with 9.10BrPC but residues close to the N and C termini of TM1 exhibited greatest quenching with 6.7BrPC (Q21W, I43W, M47W, and A51W). Conversely, a stretch of residues from A28W to I39W exhibited higher quenching with 11.12BrPC than with 6.7BrPC (Fig. 2), consistent with these residues lying close to the center of the bilayer. Thus, the differentially labeled lipids define the depth of the hydrophobic component of the bilayer centered on residues A28–I39.

Residue I57W at the carboxy-terminal extremity of TM1 provided one of the most interesting results. The emission peak position of I57W is  $340.3 \pm 0.2$  nm (Table S1), which is typical for Trp residues with access to the water. Similar values were observed for Q203W and D213W on the surface of the cytosolic domain [32,43]. The fractional quenching for this residue was very low ( $0.17 \pm 0.04$ ) and did not vary significantly with the position of the Br atoms (Fig. 2). These data suggest that I57W is exposed to a polar environment possibly contiguous with the water phase or the water-accessible glycerol moiety of the PLs [2,44–46].

We have previously identified the native, semi-conserved, Trp16 as critical for setting the gating threshold [47]. The structure of this region has not been resolved, although modeling has been undertaken [48]. MscS W240F/W251F [47] mutant channel has Trp16 as its single native Trp residue. When reconstituted with different brominated lipids, significant quenching was observed that was greatest for 6.7BrPC and least for 11.12BrPC (Fig. 2). This establishes that this critical residue is buried in the lipid bilayer.

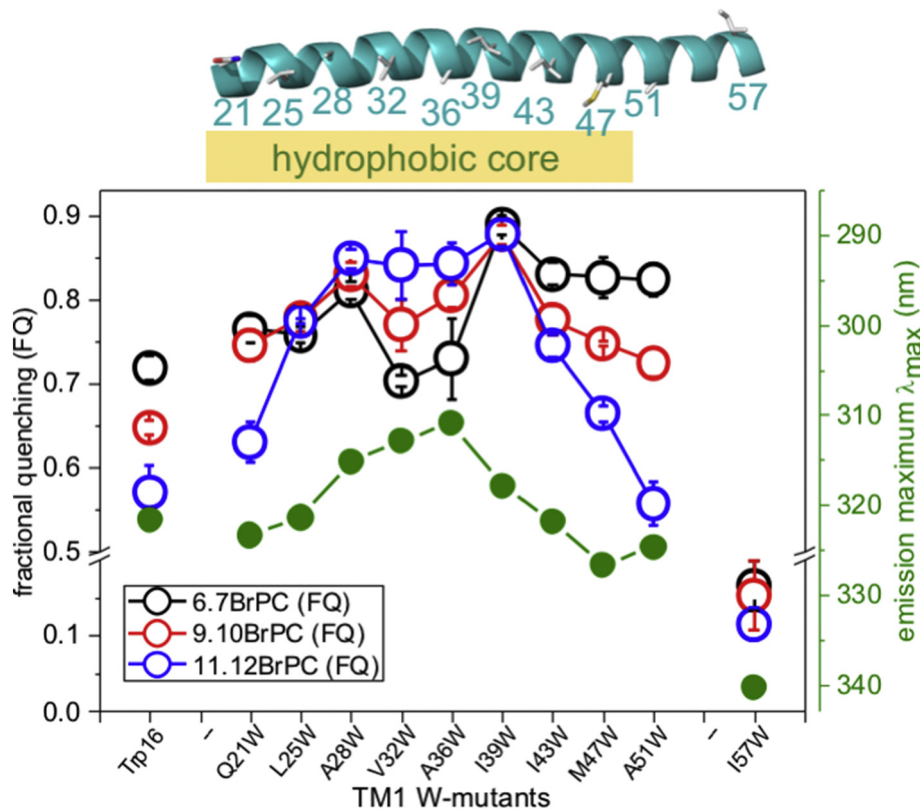


**Fig. 2.** Association of the membrane bilayer to TM1. Fractional quenching for W-mutants on TM1 are shown for reconstitutions with lipids brominated at different positions along the fatty acid chains (key: black, 6.7BrPC; red, 9.10BrPC; blue, 11.12BrPC). Emission maxima for the individual mutants are shown in green. The center of the membrane is approximately at residues A34–L35. The structure of TM1 from the MscS structure D67C (PDB: 5AJI) is shown on top indicating the hydrophobic core region of the membrane (orange). Data for Trp16 are shown on the left.

### Do lipids occupy pockets in the MscS structure?

The molecular structure of MscS exhibits grooves and pockets that are created by the TM1–2 helix pair, TM3b and the channel pore created by seven TM3a helices [34] (Fig. 1b, c). Previous work suggested that lipids might occupy the pockets and align with the hydrophobic surface of TM3b [32]. To investigate this possibility in greater depth, native residues were exchanged for Trp at positions of interest throughout TM2, TM3a, and TM3b where the amino acid side chains are predicted to project into the pockets (Fig. 1c; Fig. S1b) [32,34,35]. In addition, two mutations were created in the  $\beta$  domain (I150W and F151W) [32,34,35]. BrPC quenched residues lining the proposed pocket, with the lowest quenching observed for residues close to the carboxy-terminus of TM3b (e.g., F127W; Fig. 3;

Table S1). It was notable that I150W, which lies proximal to F127, exhibited high quenching (Table S1).

Analysis of quenching with lipids with bromine at different positions revealed that Trp residues close to the periphery of MscS (F127W, F150W, and I151W) were quenched more readily by 6.7BrPC than by 11.12BrPC. Conversely, residues lying deep within the proposed pockets (A103W and L111W) were more readily quenched by 11.12BrPC (Table S1). Residues at intermediate positions (A119W and L123W) were less affected by the position of the bromine atom in the lipid but showed a high overall level of quenching (Fig. 3; Table S1). The ratio of quenching by 11.12BrPC to quenching by 6.7BrPC indicates the positional dependence of Br/Trp interaction. This ratio is highest for L111W (1.43), lowest for F127W (0.43), with intermediate values for A119W (1.06) and L123W

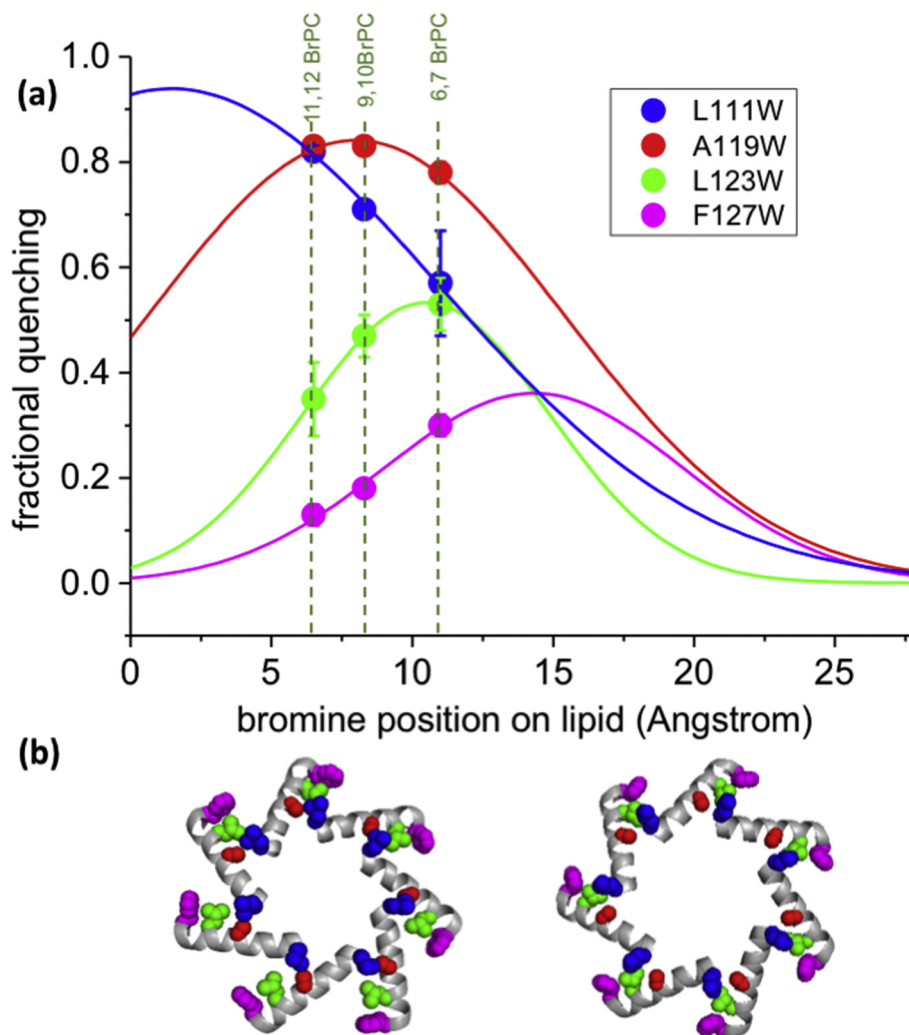


**Fig. 3.** Distance-dependent quenching of tryptophan probes located on TM3b. (a) Fractional quenching by 6.7BrPC, 9.10BrPC, and 11.12BrPC for L111W (blue), A119W (red), L123W (green), and F127W (magenta) are shown as points. These data were fitted to Gaussian curves (lines). These data suggest that the phosphate groups of the lipids are located approximately beside F127 if they adopt a stretched conformation. (b) Relative positions of residues on TM3b using same color code as in panel a: left, closed structure, 2oau; right, open structure, 5aji.

(0.66). A Gaussian distribution was fitted to the quenching data and exhibited broad profile (Fig. 3). This Gaussian distribution reflects the relative molecular movement and flexibility of probe and quencher, which broadens the effect of the intrinsically short-distance quenching mechanism. These data are consistent with lipid chains from the PLs aligning with TM3b such that their terminal methyl group closest to the pore helix (TM3a) and the charged phosphate group located on the periphery of MscS (defined by F127, I150, and F151) (Figs. 1 and S1b), which is almost perpendicular to lipids within the membrane.

We have previously characterized G113W as a fully functional Trp mutant that lies within the vestibule on the cytoplasmic side and should have least access to lipids, thereby acting as a control for the other mutants. G113W exhibited very low quenching ( $0.07 \pm 0.04$ ; Table S1) consistent with its position. Residues A94 and G101 form the TM3a inter-helix interface close to the pore entrance. Perturbation of that interface by substitution of residues with larger side chains inhibits channel function [49]. Trp mutations at these positions carry a degree of uncertainty of the position of the side chain. The  $\lambda_{\max}$  values ( $322.5 \pm 2.7$  and  $315.2 \pm 3.3$  for A94W and G101W, respectively) are intermediate between those for fully exposed and buried Trp residues (Table S1). However, fractional quenching of A94W and G101W by brominated lipids ( $0.81 \pm 0.01$  and  $0.72 \pm 0.01$ , respectively; Table S1) is consistent with high access of the Trp side chain to lipids.

Free fatty acids are expected to have a significant presence in the *E. coli* membrane, arising from lipid turnover [50]. Moreover, fatty acids are convenient mimics for known activators of MscS, for example, local anesthetics [27–29]. Interaction of free C16 fatty acids (FA) with MscS was tested by synthesis of brominated fatty acids from their equivalent C16-unsaturated precursors (see SI). Bromination was obtained at positions 4–5, 9–10, and 15–16. Reconstitution in lipid mixtures containing brominated fatty acids led to quenching of Trp residues in the pocket with similar trends to those observed for BrPC (Fig. S6). However, quenching of L111W was not significantly dependent on the position of the bromine atoms along the fatty acid chain. Control experiments show that this residue is more affected than A119W and L123W by the solvent, methanol, that was used to introduce the fatty acids. Methanol caused a red-shift and intensity increase for L111W (Fig. S6). These data are consistent with fatty acids aligning in the pockets with their carboxylate groups oriented similar to the PL headgroups.

### Defining the dimensions of the lipid pocket using competition experiments

Competition experiments utilizing the quenching assay with brominated lipids are a useful tool to investigate the dimensions of the proposed lipid

pocket. Cardiolipin (CL) is present at a low percentage in *E. coli* membranes [51]. Uniquely, it has four fatty acid chains per headgroup, and the headgroup is diminished due to the absence of choline or a related base. Cholesterol (Chol) is not synthesized by bacteria but can be absorbed from the mammalian host and incorporated into membranes [52]. In this study, Chol is a rigid volumetric probe as it associates only poorly with the brominated lipids with bromine atoms in both chains [38]. Thus, MscS Trp mutants A119W and L111W were reconstituted into mixtures of either CL or Chol where these lipids replaced part of the BrPC (ratio BrPC:CL or Chol, 67:33). Intrusion into the pockets by either CL or Chol would replace brominated lipid chains and hence reduce the quenching. A clear de-quenching of about 25% was observed for mutants A119W and L111W when CL partially replaced BrPC in the reconstitution lipids (Fig. S7), indicating that CL lipid chains can penetrate the pockets. In contrast, the presence of Chol did not lead to measurable de-quenching (Fig. S7), suggesting that Chol is excluded.

Branched lipids have previously been used to analyze the mechanism of the TRAAK channel [53]. It was demonstrated that branched chain PLs could not readily penetrate the “pocket” in TRAAK, and consequently, the channel remained conductive when reconstituted in the presence of these lipids [53]. We thus sought to determine whether branched chain PLs would penetrate the pockets of MscS. Mutant A94W was chosen for analysis on the basis that it is one of the Trp residues most remote from the end of TM3b (see above, Fig. 3). MscS A94W was reconstituted into different ratios of the branched PL, 1,2-diphytanoyl-*sn*-glycero-3-phosphocholine (4Me-16:0-PC), and BrPC and the fluorescence intensities were measured (Fig. 4) using mixtures of DOPC and BrPC as controls. Mixtures of BrPC with branched lipids quench to a similar degree as BrPC/DOPC mixtures as control (Fig. 4; compare red and black dots), indicating that these lipids readily access the pocket. However, when WT MscS was reconstituted into the branched lipid (4Me-16:0-PC) as the sole lipid in liposomes the channels retained a “flickery” state with fast openings and closings after pressure was released ( $n = 12$ ; Fig. 4, inset; Fig. S8), rather than the expected closure. This behavior is reminiscent of that observed with polyunsaturated PLs [30]. Our data suggest that branched lipids can access the pockets and have there a profound effect on gating.

### Do short chain PLs modulate MscS structure?

Previously, mass spectrometry revealed the presence of short-chain PLs in the purified MscS protein-detergent complex [32]. In particular, PG C30:1, PE C14:0/C14:0, and PE C16:1/C14:0 were identified. These lipids are at low abundance in *E. coli* membranes [54]. Other studies have implied

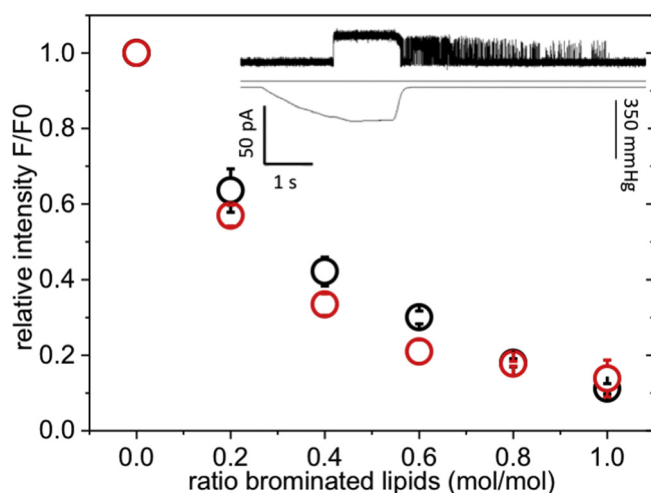


**Fig. 4.** Access of branched lipids to the pockets of MscS. Relative fluorescence intensity of MscS  $\Delta$ W A94W in mixtures of 4Me-16:0-PC with BrPC (red) or DOPC with BrPC (black) showing the competition of the branched lipid with the normal un-branched lipid within the pore. The fluorescence intensities were normalized to the sample reconstituted in 100% non-brominated lipid. The inset shows a representative electrophysiological trace (top) of MscS reconstituted into branched lipids with the corresponding pressure trace (bottom). A more detailed description and control is given in the SI (Fig. S8).

conformational changes in the large mechanosensitive channel, MscL, induced by reconstitution in short-chain PLs [55]. The ability of short-chain PLs to bind preferentially to MscS was therefore investigated. Purified MscS A119W and L111W channels were reconstituted in mixtures of BrPC (diBr C18) and either C14:1 or C18:1 and the fluorescence properties determined. Preferential binding of the C14:1/C14:1 lipid would be evident as reduced quenching by the brominated lipid. However, no significant difference in quenching was observed between C14:1 and C18:1 PLs with a relative quenching constant of  $K_{C14/C18} = 0.9 \pm 0.1$  for A119W (Fig. S9a,b). A notable effect of C14:1 lipids, however, was a change in the quantum yield for A119W. Normalizing the fluorescence intensity for A119W to protein concentration revealed an  $\sim 20\%$  lowering of this parameter for protein reconstituted in PC C14:1/C14:1 compared with PC C18:1/C18:1 (Fig. S9c). No change in quantum yield was observed in experiments with L111W (Fig. S9d). These data are consistent with conformational changes, possibly as a result of membrane thinning in PC C14:1/C14:1 bilayers.

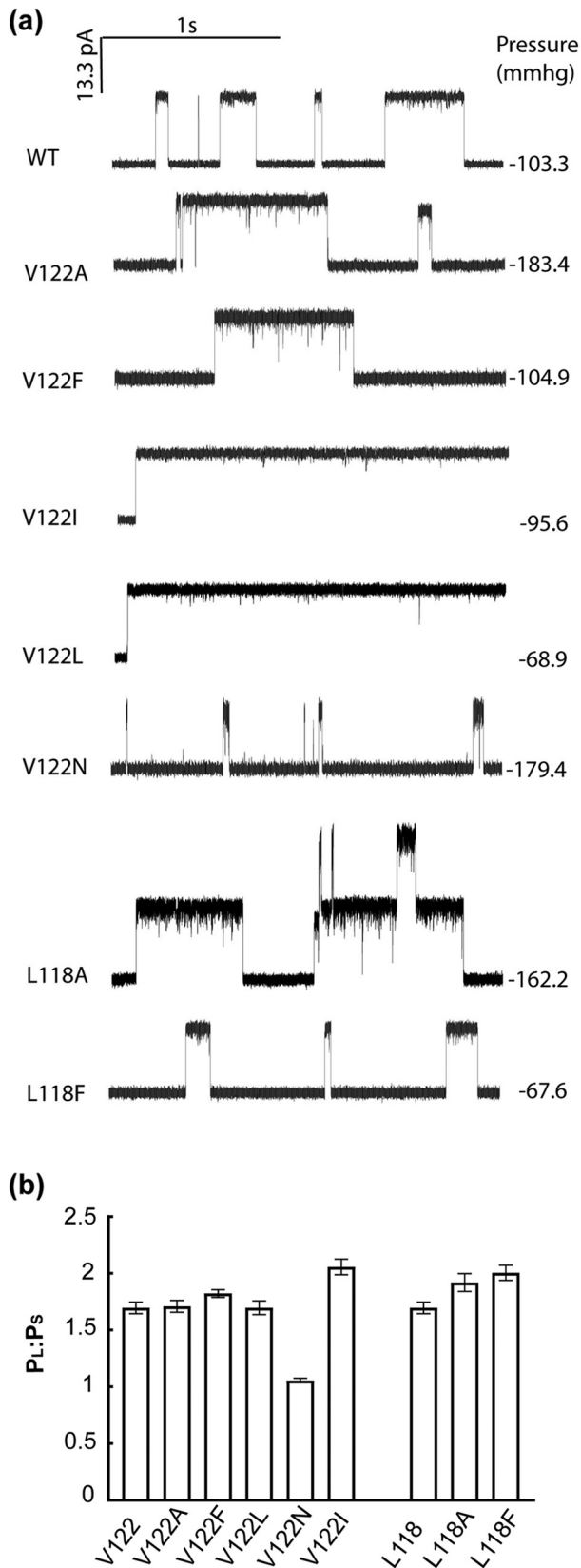
### The role of Arg46 and Arg59 in gating MscS

TM1 and TM2 are notable for transmembrane helices by the presence of basic residues Arg46, Arg59, and Arg74 [34,56,57]. Positioning of the bilayer lipids on TM1 and in the pockets may be fine regulated by charges on the sensor paddles. Indeed these residues are critical in defining the lipid exposed region of MscS using the OPM modeling [36]. Thus, we sought to investigate mutants in which the charges were neutralized. Previous work established that R46N mutants exhibited essentially wild type behavior [56]. Insertion of a hydrophobic residue (Leu) at this position (R46L) caused the channel to be more difficult to gate ( $P_L/P_S = 1.13 \pm 0.04$ ) without significantly affecting either the conductance or the stability of the

open state (Fig. S10a). Conversely, substitution of R59 by leucine caused a strong GOF phenotype that manifested as a  $P_L/P_S$  ratio =  $2.05 \pm 0.10$  in patch clamp analysis (Fig. S10a) and growth inhibition during expression (Fig. S10c). Thus, replacement of Arg residues 46 and 59 by Leu significantly affects the tension sensing of the resultant channels.

### Mutations in TM3b modulate gating and open-state stability

TM3b is a relatively well-conserved amphipathic helix (Fig. S2) in which the hydrophobic residues are orientated into the proposed pocket and the hydrophilic residues orientated to the  $\beta$  domain. Our Trp mutations on TM3b led to significant changes in channel activity in physiological assays (Fig. S3–4), suggesting that either the bulk or the polarity of the side chain impaired channel function. Work by others has also established the sensitivity of this helix to mutagenesis with amino acid replacements causing altered gating and stability of MscS [58–60]. To extend this analysis, we selected three positions in native MscS to mutate to alternative residues to complement the Trp mutations in this study (Fig. S11). Residues L118, V122, and M126 are on the same face of the helix as the Trp residues, and we changed either charge or the volume of the residue. Polar insertions at position 118, 122, and 126 caused impaired channel activity in downshock assays (Fig. S11a). In electrophysiological assays, no channels were observed for L118Q and M126R despite good expression of both proteins (Fig. S11b). The V122N channel opened at pressures similar to those that gated MscL (Table S2; Fig. 5) and channel openings were of short duration (Fig. 5). Hydrophobic substitutions at positions 118 and 122 also created channels with substantially modified behavior (Figs. 5 and S12). Both L118A and L118F exhibited increased pressure sensitivity but exhibited essentially normal conductance and openings [60]. Similarly, V122F and V122A mutants



exhibited only modest changes in channel properties (Fig. 5 and Table S2). In contrast, V122L and V122I exhibited wild type and increased pressure sensitivity, respectively (Figs. 5 and Table S2), but exhibited a sustained open state that did not close upon sustained stimuli as rapidly as the wild type (Fig. S12). Thus, subtle changes in side chain structure at V122 modulate channel behavior.

## Discussion

Lipid–protein interactions are often difficult to investigate. Elegant analyses by Marsh [11,40,61] have shown that, for the majority of membrane proteins, lipid headgroup packing against the surface of the protein defines the number of lipids immediately surrounding the protein complex. Recent work has shown that hydrogen networks between lipid headgroups and polar residues determine the protein conformation [3,13]. However, both MscS and MscL are inhibited by insertion of polar residues at the periphery of the protein close to the lipid headgroups [62,63]. Indeed, MscS has a distinctly asymmetric distribution of charged and polar residues in TM1 and TM2, the helix pair that have the potential to interact directly with lipids (Fig. S1c; see below). Our analysis suggests that the surface of MscS between residues 21 and 47 is buried in the lipid bilayer, as predicted by the OPM model for a simple planar bilayer. Brominated lipids quench Trp residues positioned from 21 to 47 of TM1, consistent with a hydrophobic depth of 30 Å [46], with the center around residue 32–36 (Fig. 2). I57W, which lies close to the TM1–2 turn, appears to be predominantly in an aqueous environment. However, lipid chains can interact with I150 and the surface of TM3b, which lie below I57W and distant to the planar bilayer contact zone. These data would support a model for the lipid–protein interactions in which a distortion or bulge of the PLs occurs, which was predicted for MscS [64] and reported for the mechanosensitive Piezo1 channel [12,65] (see below).

**Fig. 5.** Electrophysiological characterization of mutants at highly conserved positions in TM3b. (a) Representative traces of single-substituted mutants of V122 and L118 in *E. coli* MscS. A scale bar is presented at top left of the traces. Note that absolute pressure values at which channels open differ between patches due to variation in patch geometry. Therefore, an internal reference, MscL channel opening, is used as a reference and the ratio expressed as P<sub>L</sub>:P<sub>S</sub>, which is ~1.5 for wild type MscS channels. (b) MscL channel opening is used as an internal standard to compare mehanosensitivity between different mutants. The ratio P<sub>L</sub>:P<sub>S</sub> values for the TM3b mutants. Mutants with ratios greater than V122 (1.7) are more sensitive to pressure and, conversely, those with ratios less than 1.7 are less sensitive to pressure.

Lipid chains have great fluidity and will tend to fill crevices in the lipid-exposed surfaces of a membrane protein. The molecular dimensions of the TM1–2 paddles of MscS and their mobility create variable crevices into which lipid chains can insert (Fig. 1). Viewing molecular models of MscS one can see a clear pocket in the structure that exposes L111 to the environment (Fig. 1b). This pocket is lined with the hydrophobic residues of TM3b and terminates with F127, F151, and I150 (Figs. 1b and S1b). The data presented here are consistent with deep penetration of the pockets by lipid chains (Fig. 3). The position-dependent quenching data (Fig. 3a and Table S1) are consistent with the negatively charged phosphate group of the PL at the last turn of TM3b close to F127. Similarly, the quenching of a I150W, F127W, and F151W indicate lipid chains freely access the volume immediately above TM3b in the pockets of MscS (Fig. 1c). This is clearly inconsistent with a simple planar bilayer as envisaged by the OPM model. The two possibilities are compatible with some distortion of the bilayer, as recently seen with Piezo [12,65]. One of the fascinating features of MscS is that the distribution of charged or polar residues in the TM1 and TM2 helices that can potentially interact with the lipid bilayer is asymmetrically distributed—there are few on the periplasmic ends of the helices and many on the cytoplasmic ends (Fig. S1c). Furthermore, insertion of polar residues at the periplasmic ends of TM1 decreases the sensitivity to membrane tension (i.e., making the channels less active) [62], which would be compatible with the cytoplasmic and periplasmic ends of TM1 having very different lipid packing. A simple explanation for the cluster of polar residues at the cytoplasmic ends of TM1 and TM2 would be that they organize the headgroups of the “non-simple bilayer” lipids to ensure the pockets are occupied by lipid chains.

The presence of basic residues in TM1 and TM2 was highlighted as an unusual feature of this membrane protein, and it was proposed that this might lead to voltage sensing [34]. Significant doubt has been cast on this role for the Arg residues in TM1 [56]. However, our data do point to a critical role for these residues in gating since neutralization of the charges (R46L and R59L) has profound, but opposite, effects on channel gating (Fig. S10). It seems plausible that these mutations perturb the headgroup interaction with MscS and may affect lipid packing or orientation in the pockets. It is notable either Asp or Glu can replace Arg, suggesting that the capacity to interact with headgroups of lipids is important. The change from a hydrophilic to hydrophobic residue at R46 and R59 could have a more profound impact in such a scenario.

Conservation of the hydrophobic TM3b surface is clearly important, but our study also suggests further complexity. Not only do single polar residues cause profound loss of activity (Table S2 and Fig. 5) but relatively conservative changes that preserve

the hydrophobicity affect the rate of loss of channel activity during sustained stimulus (Fig. 5, Table S2, and Fig. S12) (see also Refs. [58–60,66]). Val122 may have a critical role in gating. Introduction of other hydrophobic residues by mutation causes major changes in tension sensing and open stability (Fig. 5). These effects of mutations at Val122 are reminiscent of substitutions at Leu 596 in TrpV4 [67]. In the TrpV4 study, mutations that decreased the hydrophobicity caused loss of function and this effect was speculated to arise from the modified lipid interactions. Intriguingly, TrpV4 L596I was a gain-of-function mutant. The only structural change in the mutants was the organization of the methyl groups on the respective amino acid side chains, with the consequence that the substituted amino acid side chain is buried more deeply in the bilayer [67,68]. In MscS, the profound change in character from Val122 to Leu or Ile may similarly relate to the organization of the side chain (indeed even replacement of Leu with Ala causes a change in rate at which channels closed upon continued stimulus (entry to the “tension-insensitive inactivated state” [69] (Table S2 and Fig. S11)).

Our analysis of MscS-lipid interactions provides insights and poses new questions. Previously, Trp16 in the native MscS has been shown to be important for tension sensing [47]. This residue, we have shown here, is likely to be buried in the periplasmic leaflet of the bilayer (Fig. 2). The periplasmic mouth of the MscS pore lies well below the surface of the planar bilayer, indeed close to the center of the bilayer. Correspondingly, the hydrophobic pocket lies adjacent to and below the cytoplasmic leaflet of the bilayer. One is consistently drawn to the idea that there is deformation of the bilayer at the cytoplasmic surface, as in the case of Piezo1 [12]. In the latter case, the deformation amplifies the sensitivity of the channel to membrane tension. The effects of mutations in TM1 (R46L and R59L) and in TM3b on tension sensitivity and the stability of the open state would fit with a role for these structural elements in stabilizing the deformation. It is exciting to note that the pattern of critical penetration of the channel structure by lipids is now becoming a common mechanistic element [67,68] and may be the site of action of lipophilic drugs [70]. The analogies of the effects of V122 mutations to the dependence of the mechanism of TrpV4 on specific side chain structures are supportive of commonality in mechanistic features. Our data and those of Malcolm and Blount [60] identified residues in TM3b where even subtle changes affect the critical properties of the channel. This is also seen from the influence of reconstitution of the channel into branched-chain lipids, which led to sustained gating events after pressure had been released (Fig. 4). Thus, the dimensions of the relationship between lipids and MscS structure outstrip the simple planar

bilayer evident in parts of TM1 and extend to the lipids that occupy the pockets.

## Methods

### Materials

Dodecylmaltoside (DDM) was obtained from Glycon (Germany). The PLs 1,2-dioleoyl-sn-glycero-3-phosphocholine (DOPC), 1,2-di-(9Z-tetradecenoyl)-sn-glycero-3-phosphocholine (PC C14:1/C14:1), 1-oleoyl-2-palmitoyl-sn-glycero-3-phosphocholine (POPC), 1-palmitoyl-2-(6,7-dibromo)stearoyl-sn-glycero-3-phosphocholine (6.7BrPC), 1-palmitoyl-2-(9,10-dibromo)stearoyl-sn-glycero-3-phosphocholine (9.10BrPC), 1-palmitoyl-2-(11,12-dibromo)stearoyl-sn-glycero-3-phosphocholine (11.12BrPC), and 4Me-16:0-PC were purchased from Avanti (Alabaster). DOPC was brominated as described earlier [32,71] resulting in 1,2-di-(9,10-dibromo)stearoyl-sn-glycero-3-phosphocholine (BrPC). 4,5 (4.5BrFA), 9,10 (9.10BrFA), and 15,16 (15.16BrFA) dibromopalmitic acid were synthesized as described in the SI. All other chemicals were obtained from Sigma.

### Mutagenesis and functional assays

As template for all Trp substitution mutants in this study, the tryptophan-free MscS W16Y/W240F/W251F in a pTrc99A expression vector was used, which has been proven stable and functional [47]. Mutants were made with the Stratagene QuikChange protocol and were confirmed by sequencing (Source Bioscience, Nottingham). As functional assay for the mutant forms of MscS a hypo-osmotic downshock was performed as described earlier [49,72]. For this MscS, constructs were transformed into *E. coli* strain MJF612 (Frag1  $\Delta$ mscL::cm,  $\Delta$ mscS,  $\Delta$ mscK::kan,  $\Delta$ ybdG::apr) [73] and grown in Luria–Bertani (LB) medium (10 g/L tryptone, 5 g/L NaCl, 5 g/L yeast extract) containing additional 0.5 M NaCl at 37 °C. At an OD<sub>650</sub> = 0.2 until 0.3 expression was induced with 0.3 mM IPTG in parallel with noninduced samples. Samples were then 10 times diluted into LB medium (shock medium) as well as LB medium + 0.5 M NaCl (control medium). After incubation for 10 min at 37 °C, serial dilutions were made and spread on agar plates made from control or shock medium, respectively. Colonies were counted after incubation overnight at 37 °C, and percent survival was calculated relative to the control plates.

The Arg substitution mutants were created in a wild-type clone of *mscS* in the same pTrc99A expression vector used for the mutants described above [72]. These mutants were analyzed functionally as previously described using strain MJF641 as the host and with a downshock from LB + 0.3 M NaCl to LB medium [49].

### Purification of MscS

MscS, solubilized in 1% DDM, was purified as described previously [43,47,74] in a two-step purification. The C-terminal His6-tag was bound by a nickel-nitrilotriacetic (Ni-NTA) agarose column in the first step. MscS was further purified and the heptameric complex was separated by size exclusion chromatography on a Superdex 200 10/300 column (GE Healthcare) with a buffer containing 0.03% DDM, 50 mM sodium phosphate (pH 7.5), and 150 mM NaCl.

### Reconstitution for electrophysiology

Liposomes with a branched lipid (4Me-16:0-PC) were made using a sucrose method [75]. Briefly, 2 mg of the lipid in chloroform was dried under N<sub>2</sub>. The lipid film was rehydrated with 1 ml of 0.4 M sucrose and incubated for 3 h at 45 °C. Purified MscSWT was added to achieve a protein/lipid ratio (mol complex/mol lipid) of 1:500, and the solution was shaken gently for 3 h at room temperature. Then about 200-mg biobeads (Anatrace) were added to the mixture and gently shaken overnight.

### Electrophysiology

Giant spheroplasts from *E. coli* MJF429 strain (Frag1,  $\Delta$ mscS,  $\Delta$ mscK::kan) transformed with MscS constructs in pTrc 99A vector, whose expression was induced with 1.0 mM IPTG, were generated and used in patch-clamp recordings as described previously [27,76]. Excised, inside-out patches were examined at room temperature. Patch buffers used contained 200 mM KCl, 90 mM MgCl<sub>2</sub>, 10 mM CaCl<sub>2</sub>, and 5 mM Hepes (Sigma, St. Louis, MO, USA) with pH adjusted to 8.0. Data were acquired at a sampling rate of 20 kHz with a 5-kHz filter, using an AxoPatch 200B amplifier in conjunction with Axoscope software (Axon Instruments, Union City, CA, USA). A piezoelectric pressure transducer (World Precision Instruments, Sarasota, FL, USA) was used to monitor the pressure introduced to patch membrane by suction throughout the experiments. Data analysis was performed using Clampfit 10.6 (Axon Instruments). Identical conditions were used to analyze purified channels reconstituted into lipids.

### Reconstitution and fluorescence spectroscopy

Purified MscS was reconstituted by dilution of mixtures of MscS, lipids, and detergent under the critical micellar concentration as described earlier [32]. Different variants of phosphatidylcholine, as listed in the Materials section and specified in the Result section, were used. Films of 2  $\mu$ mol lipids were formed from chloroform solutions in thin-walled glass tubes using a nitrogen stream and then

desiccation overnight at 4 °C. Lipids were suspended in 1.6 ml reconstitution buffer containing 40 mM Hepes (pH 7.2), 100 mM KCl, 1 mM EGTA, and 15 mM sodium cholate by warming the tube for 20 s in warm water, vortexing for 5 min, and subjecting to ultrasonication for 10 min (Fisher Scientific, model FB15046). 0.64 nmol MscS (monomer) was then mixed with 50  $\mu$ l of lipid solution (64 nmol) and incubated at room temperature for 15 min. Reconstitution from cholate by dilution gives a homogeneous mixture of lipid and protein in the form of large membrane vesicles [77], which was confirmed by transmission electron microscopy (Fig. S5).

For assay, 30  $\mu$ l of this mixture was then added to 600  $\mu$ l of measuring buffer (as reconstitution buffer but without sodium cholate) in a stirred quartz cell (4  $\times$  4-mm light path; Hellma). After 5-min incubation at 20 °C, fluorescence measurements were started in a FLS920 spectrometer (Edinburgh Instruments) with an excitation wavelength of 295 nm (slit width 3 nm) and an emission range from 300 to 420 nm (slit width 7 nm) and excitation and emission polarizers set to 90° and 0°, respectively. Spectra were corrected by similar samples containing only lipids but no MscS. Experiments with brominated and non-brominated lipids at different ratios were prepared as follows [71]: Solubilized solutions of the required lipids were made up as described above. Then 100  $\mu$ l each of brominated and non-brominated lipid mixtures at different mol-ratios was prepared and incubated for 30 min at 50 °C with gentle shaking. After cooling to room temperature, 50  $\mu$ l of each lipid mixture was mixed with MscS and the experiment was proceeded as described above.

Mixtures of CL or Chol with BrPC were made by mixing the chloroform solutions to result in a lipid films of 2  $\mu$ mol and 33% (mol/mol total lipid), respectively. Solubilized mixtures of these lipids were then made as described for the pure lipids above. To study the effect of bromination at different positions along the fatty acid chains, 6.7BrPC, 9.10BrPC, and 11.12BrPC were used together with POPC as non-brominated reference. The brominated fatty acids 4,5 (4.5BrFA), 9,10 (9.10BrFA), and 15,16 (15.16BrFA) dibromopalmitic acid were synthesized as described in SI and added as stock solutions in methanol to MscS mutants L111W, A119W, and L123W reconstituted in DOPC. Fluorescence emission spectra before and after addition were recorded and compared. The final concentration of methanol was below 1%. As controls, non-brominated palmitic acid or the solvent only was added.

### Analysis of fluorescence experiments

Fractional quenching was determined as  $FrQ = (F_0 - F)/F_0$ , where  $F_0$  is the fluorescence intensity at 340 nm for the sample containing 100% non-

brominated lipids, and  $F$  is the intensity for the sample containing 100% brominated lipids.

Data of fluorescence experiments in lipid mixtures were analyzed following the procedures developed by Carney and co-workers [71]:

Relative fluorescence intensities,  $F$ , were plotted against the mole fraction of brominated lipids,  $x_{Br}$ , and fitted with following equation using the software Origin 8.0:

$$F = F_{\min} + (1 - F_{\min})(1 - x_{Br})^n$$

In this equation,  $F_{\min}$  is the fluorescence intensity in BrPC, while  $n$  is the number of lattice sites for binding of lipids close enough to the fluorescence probe to cause quenching. These parameters were fitted. Using  $n$  determined from experiments in mixtures of DOPC and BrPC, the relative binding constant,  $K_{C14/C18}$ , for the short chain lipid PC C14:1/C14:1 was fitted with following equation:

$$F = F_{\min} + (1 - F_{\min}) \left[ 1 - \left( \frac{x_{Br}}{x_{Br} + K_{C14/C18}(1 - x_{Br})} \right) \right]^n$$

### Electron microscopy

Purified MscS WT was reconstituted as described in the reconstitution for fluorescence spectroscopy section. The sample was then incubated for 1 min on carbon coated copper grids (400 mesh, Plano, Germany) which were beforehand freshly glow discharged. The excess was removed with a filter paper, and the grid was then washed three times with water and three times with 2% uranyl acetate. The last cycle of staining solution was left for 5 min on the grid and was then removed with filter paper. After drying, the grids were imaged in a FEI Tecnai T12 Spirit transmission electron microscope equipped with an Eagle detector at 120 kV. A magnification of 52,000, a defocus of 1  $\mu$ m, and a total electron dose of 30 electrons/ $\text{Å}^2$  were used.

### Acknowledgments

The authors are grateful to Tony Lee (Southampton) and Jim Naismith (St Andrews and Oxford) for helpful discussions; we also thank Dr Irene Iscla (UT Southwestern) for discussions and critical reading of the manuscript. I.R.B., S.M., A.R., T.R., and S.B. were supported by a Wellcome Programme Grant (WT092552MA); H.G. and C.K. were funded by the EU FP7 ITN programme NICHE. The MscS F151W mutant was created by N. J. Hayward during his PhD

studies at the University of Aberdeen. We thank Vanessa Flegler for assistance in the electron microscopy experiment. I.R.B. was a recipient of a Leverhulme Emeritus Research Fellowship and a CEMI research grant from Caltech; P.B. was supported by Grant I-1420 of the Welch Foundation and Grant GM121780 from the National Institutes of Health. The content is solely the responsibility of the authors and does not necessarily represent the official views of the National Institutes of Health or other funding organizations.

**Author Contributions:** T.R., A.R., L.Y., S.B., C.K. and H.G. conducted experimental work, T.R. and I.R.B. wrote the original draft, T.R. purified and reconstituted the protein, conducted fluorescence studies and analysed the data, A.R., L.Y., H.G., and S.B. conducted electrophysiology and analysed the data, A.R., H.G., S. B., and L.Y. created mutants and analysed their properties, T.R., P.B., L.Y., S.M. and I.R.B. reviewed and edited the manuscript, S.M. and S.J.C. supervised and undertook project administration, I.R.B., T.R., S.M., and S.J.C. developed the concept, I.R.B., S.M., S.J.C. and P.B. acquired funds.

**Declaration of Competing Interest:** The authors are not aware of any competing interests affecting this work.

## Appendix A. Supplementary data

Supplementary data to this article can be found online at <https://doi.org/10.1016/j.jmb.2019.05.043>.

*Received 20 March 2019;*

*Received in revised form 14 May 2019;*

*Available online 04 June 2019*

### **Keywords:**

lipid–protein interaction;  
fluorescence quenching;  
brominated lipids;  
tension sensing;  
electrophysiology

Present address: T. Rasmussen and A. Rasmussen, Institute for Biochemistry, Rudolf-Virchow-Zentrum, University of Würzburg, Josef-Schneider-Str. 2, 97080 Würzburg, Germany.

Present address: C. Kaul, United Initiators GmbH, Dr.-Gustav-Adolph-Str. 3, 82049 Pullach, Germany.

Present address: S. Black, Division of Structural Biology, University of Oxford Henry Wellcome Building for Genomic Medicine, Oxford, OX3 7BN, UK.

Present address: H. Galbiati, Sars International Centre for Marine Molecular Biology Thormøhlens gate 55, N-5006 Bergen, Norway.

### **Abbreviations used:**

DOPC, 1,2-dioleoyl-sn-glycero-3-phosphocholine; POPC, 1-oleoyl-2-palmitoyl-sn-glycero-3-phosphocholine; BrPC, 1,2-di-(9,10-dibromo)stearoyl-sn-glycero-3-phosphocholine; 6.7BrPC, 1-palmitoyl-2-(6,7-dibromo)stearoyl-sn-glycero-3-phosphocholine; 9.10BrPC, 1-palmitoyl-2-(9,10-dibromo)stearoyl-sn-glycero-3-phosphocholine; 11.12BrPC, 1-palmitoyl-2-(11,12-dibromo)stearoyl-sn-glycero-3-phosphocholine; Chol, cholesterol; PL, phospholipid; CL, cardiolipin; 4Me-16:0-PC, 1,2-diphytanoyl-sn-glycero-3-phosphocholine; 4.5BrFA, 4,5 dibromopalmitic acid; 9.10BrFA, 9,10 dibromopalmitic acid; 15.16BrFA, 15,16 dibromopalmitic acid.

## References

- [1] F. Cymer, G. von Heijne, S.H. White, Mechanisms of integral membrane protein insertion and folding, *J. Mol. Biol.* 427 (2015) 999–1022.
- [2] A.G. Lee, How lipids and proteins interact in a membrane: a molecular approach, *Mol. BioSyst.* 1 (2005) 203–212.
- [3] C. Martens, M. Shekhar, A.J. Borysik, A.M. Lau, E. Reading, E. Tajkhorshid, et al., Direct protein–lipid interactions shape the conformational landscape of secondary transporters, *Nat. Commun.* 9 (2018) 4151.
- [4] A.M. Powl, J.M. East, A.G. Lee, Lipid–protein interactions studied by introduction of a tryptophan residue: the mechanosensitive channel MscL, *Biochemistry.* 42 (2003) 14306–14317.
- [5] A.M. Powl, J.N. Wright, J.M. East, A.G. Lee, Identification of the hydrophobic thickness of a membrane protein using fluorescence spectroscopy: studies with the mechanosensitive channel MscL, *Biochemistry.* 44 (2005) 5713–5721.
- [6] D. Marsh, Lipid–protein interactions and heterogeneous lipid distribution in membranes, *Mol. Membr. Biol.* 12 (1995) 59–64.
- [7] D. Marsh, Lipid interactions with transmembrane proteins, *Cellular and molecular life sciences : CMLS.* 60 (2003) 1575–1580.
- [8] D. Marsh, T. Pali, The protein–lipid interface: perspectives from magnetic resonance and crystal structures, *Biochim. Biophys. Acta* 1666 (2004) 118–141.
- [9] T. Pali, D. Bashtovyy, D. Marsh, Stoichiometry of lipid interactions with transmembrane proteins—deduced from the 3D structures, *Protein Sci.* 15 (2006) 1153–1161.
- [10] D. Marsh, Energetics of hydrophobic matching in lipid–protein interactions, *Biophys. J.* 94 (2008) 3996–4013.
- [11] D. Marsh, T. Pali, Orientation and conformation of lipids in crystals of transmembrane proteins, *Eur. Biophys. J.* 42 (2013) 119–146.
- [12] C.A. Haselwandter, R. MacKinnon, Piezo's membrane footprint and its contribution to mechanosensitivity, *Elife.* 7 (2018).
- [13] C. Martens, R.A. Stein, M. Masureel, A. Roth, S. Mishra, R. Dawaliby, et al., Lipids modulate the conformational dynamics of a secondary multidrug transporter, *Nat. Struct. Mol. Biol.* 23 (2016) 744–751.
- [14] D. Marsh, L.I. Horvath, Structure, dynamics and composition of the lipid–protein interface. Perspectives from spin-labelling, *Biochim. Biophys. Acta* 1376 (1998) 267–296.

- [15] S.I. Sukharev, P. Blount, B. Martinac, F.R. Blattner, C. Kung, A large-conductance mechanosensitive channel in *E. coli* encoded by *mscL* alone, *Nature*. 368 (1994) 265–268.
- [16] S.I. Sukharev, W.J. Sigurdson, C. Kung, F. Sachs, Energetic and spatial parameters for gating of the bacterial large conductance mechanosensitive channel, *MscL*, *J Gen Physiol*. 113 (1999) 525–540.
- [17] J. Teng, S. Loukin, A. Anishkin, C. Kung, The force-from-lipid (FFL) principle of mechanosensitivity, at large and in elements, *Pflugers Arch*. 467 (2015) 27–37.
- [18] I.R. Booth, P. Blount, The MscS and MscL families of mechanosensitive channels act as microbial emergency release valves, *J. Bacteriol*. 194 (2012) 4802–4809.
- [19] C.D. Cox, N. Bavi, B. Martinac, Bacterial mechanosensors, *Annu. Rev. Physiol*. 80 (2018) 71–93.
- [20] C. Kung, A possible unifying principle for mechanosensation, *Nature*. 436 (2005) 647–654.
- [21] M. Bialecka-Fornal, H.J. Lee, R. Phillips, The rate of osmotic downshock determines the survival probability of bacterial mechanosensitive channel mutants, *J. Bacteriol*. 197 (2015) 231–237.
- [22] I.R. Booth, S. Miller, A. Rasmussen, T. Rasmussen, M.D. Edwards, Mechanosensitive channels: their mechanisms and roles in preserving bacterial ultrastructure during adaptation to environmental change, in: W. El-Sharoud (Ed.), *Bacterial Physiology a Molecular Approach*, Springer, Berlin, Heidelberg 2008, pp. 73–96.
- [23] M. Reuter, N.J. Hayward, S.S. Black, S. Miller, D.T. Dryden, I. R. Booth, Mechanosensitive channels and bacterial cell wall integrity: does life end with a bang or a whimper? *J. R. Soc. Interface* 11 (2014) 20130850.
- [24] M. Boer, A. Anishkin, S. Sukharev, Adaptive MscS gating in the osmotic permeability response in *E. coli*: the question of time, *Biochemistry*. 50 (2011) 4087–4096.
- [25] I.R. Booth, Bacterial mechanosensitive channels: progress towards an understanding of their roles in cell physiology, *Curr. Opin. Microbiol*. 18 (2014) 16–22.
- [26] I.R. Booth, T. Rasmussen, M.D. Edwards, S. Black, A. Rasmussen, W. Bartlett, et al., Sensing bilayer tension: bacterial mechanosensitive channels and their gating mechanisms, *Biochem. Soc. Trans*. 39 (2011) 733–740.
- [27] B. Martinac, J. Adler, C. Kung, Mechanosensitive ion channels of *E. coli* activated by amphipaths, *Nature*. 348 (1990) 261–263.
- [28] T. Nguyen, B. Clare, W. Guo, B. Martinac, The effects of parabens on the mechanosensitive channels of *E. coli*, *Eur. Biophys. J*. 34 (2005) 389–395.
- [29] T. Nomura, C.G. Cranfield, E. Deplazes, D.M. Owen, A. Macmillan, A.R. Battle, et al., Differential effects of lipids and lyso-lipids on the mechanosensitivity of the mechanosensitive channels MscL and MscS, *Proc. Natl. Acad. Sci. U. S. A*. 109 (2012) 8770–8775.
- [30] P. Ridone, S.L. Grage, A. Patkunarajah, A.R. Battle, A.S. Ulrich, B. Martinac, "Force-from-lipids" gating of mechanosensitive channels modulated by PUFAs, *J. Mech. Behav. Biomed. Mater*. 79 (2018) 158–167.
- [31] J.H. Naismith, I.R. Booth, Bacterial mechanosensitive channels—MscS: evolution's solution to creating sensitivity in function, *Annu. Rev. Biophys*. 41 (2012) 157–177.
- [32] C. Pliotas, A.C. Dahl, T. Rasmussen, K.R. Mahendran, T.K. Smith, P. Marius, et al., The role of lipids in mechanosensation, *Nat. Struct. Mol. Biol*. 22 (2015) 991–998.
- [33] N. Bavi, C.D. Cox, E. Perozo, B. Martinac, Toward a structural blueprint for bilayer-mediated channel mechanosensitivity, *Channels (Austin)*. 11 (2017) 91–93.
- [34] R.B. Bass, P. Strop, M. Barclay, D.C. Rees, Crystal structure of *Escherichia coli* MscS, a voltage-modulated and mechanosensitive channel, *Science*. 298 (2002) 1582–1587.
- [35] W. Wang, S.S. Black, M.D. Edwards, S. Miller, E.L. Morrison, W. Bartlett, et al., The structure of an open form of an *E. coli* mechanosensitive channel at 3.45 Å resolution, *Science*. 321 (2008) 1179–1183.
- [36] M.A. Lomize, I.D. Pogozheva, H. Joo, H.I. Mosberg, A.L. Lomize, OPM database and PPM web server: resources for positioning of proteins in membranes, *Nucleic Acids Res*. 40 (2012) D370–D376.
- [37] J.M. East, A.G. Lee, Lipid selectivity of the calcium and magnesium ion dependent adenosinetriphosphatase, studied with fluorescence quenching by a brominated phospholipid, *Biochemistry*. 21 (1982) 4144–4151.
- [38] A.M. Powl, J. Carney, P. Marius, J.M. East, A.G. Lee, Lipid interactions with bacterial channels: fluorescence studies, *Biochem. Soc. Trans*. 33 (2005) 905–909.
- [39] D. Marsh, Application of electron spin resonance for investigating peptide–lipid interactions, and correlation with thermodynamics, *Biochem. Soc. Trans*. 29 (2001) 582–589.
- [40] D. Marsh, Electron spin resonance in membrane research: protein–lipid interactions, *Methods*. 46 (2008) 83–96.
- [41] H.I. Petrache, S.W. Dodd, M.F. Brown, Area per lipid and acyl length distributions in fluid phosphatidylcholines determined by <sup>2</sup>H NMR spectroscopy, *Biophys. J*. 79 (2000) 3172–3192.
- [42] E.J. Bolen, P.W. Holloway, Quenching of tryptophan fluorescence by brominated phospholipid, *Biochemistry*. 29 (1990) 9638–9643.
- [43] T. Rasmussen, A. Rasmussen, S. Singh, H. Galbati, M.D. Edwards, S. Miller, et al., Properties of the mechanosensitive channel MscS pore revealed by tryptophan scanning mutagenesis, *Biochemistry*. 54 (2015) 4519–4530.
- [44] J.A. Killian, G. von Heijne, How proteins adapt to a membrane–water interface, *Trends Biochem. Sci*. 25 (2000) 429–434.
- [45] S.H. White, W.C. Wimley, Hydrophobic interactions of peptides with membrane interfaces, *Biochim. Biophys. Acta* 1376 (1998) 339–352.
- [46] S.H. White, W.C. Wimley, Membrane protein folding and stability: physical principles, *Annu. Rev. Biophys. Biomol. Struct*. 28 (1999) 319–365.
- [47] A. Rasmussen, T. Rasmussen, M.D. Edwards, D. Schauer, U. Schumann, S. Miller, et al., The role of tryptophan residues in the function and stability of the mechanosensitive channel MscS from *Escherichia coli*, *Biochemistry*. 46 (2007) 10899–10908.
- [48] A. Anishkin, B. Akitake, S. Sukharev, Characterization of the resting MscS: modeling and analysis of the closed bacterial mechanosensitive channel of small conductance, *Biophys. J*. 94 (2008) 1252–1266.
- [49] M.D. Edwards, Y. Li, S. Kim, S. Miller, W. Bartlett, S. Black, et al., Pivotal role of the glycine-rich TM3 helix in gating the MscS mechanosensitive channel, *Nat. Struct. Mol. Biol*. 12 (2005) 113–119.
- [50] Y.M. Zhang, C.O. Rock, Membrane lipid homeostasis in bacteria, *Nat Rev Microbiol*. 6 (2008) 222–233.
- [51] T. Romantsov, Z. Guan, J.M. Wood, Cardiolipin and the osmotic stress responses of bacteria, *Biochim. Biophys. Acta* 1788 (2009) 2092–2100.

- [52] A. Toledo, Z. Huang, J.L. Coleman, E. London, J.L. Benach, Lipid rafts can form in the inner and outer membranes of *Borrelia burgdorferi* and have different properties and associated proteins, *Mol. Microbiol.* 108 (2018) 63–76.
- [53] S.G. Brohawn, E.B. Campbell, R. MacKinnon, Physical mechanism for gating and mechanosensitivity of the human TRAAK K<sup>+</sup> channel, *Nature*. 516 (2014) 126–130.
- [54] D. Oursel, C. Loutelier-Bourhis, N. Orange, S. Chevalier, V. Norris, C.M. Lange, Lipid composition of membranes of *Escherichia coli* by liquid chromatography/tandem mass spectrometry using negative electrospray ionization, *Rapid Commun. Mass Spectrom.* 21 (2007) 1721–1728.
- [55] E. Perozo, D.C. Rees, Structure and mechanism in prokaryotic mechanosensitive channels, *Curr. Opin. Struct. Biol.* 13 (2003) 432–442.
- [56] T. Nomura, M. Sokabe, K. Yoshimura, Voltage-dependent inactivation of MscS occurs independently of the positively charged residues in the transmembrane domain, *Biomed. Res. Int.* 2016 (2016), 2401657.
- [57] M.B. Ulmschneider, J.P. Ulmschneider, J.A. Freitas, G. von Heijne, D.J. Tobias, S.H. White, Transmembrane helices containing a charged arginine are thermodynamically stable, *Eur. Biophys. J.* 46 (2017) 627–637.
- [58] B. Akitake, A. Anishkin, N. Liu, S. Sukharev, Straightening and sequential buckling of the pore-lining helices define the gating cycle of MscS, *Nat. Struct. Mol. Biol.* 14 (2007) 1141–1149.
- [59] P. Koprowski, W. Grajkowski, E.Y. Isacoff, A. Kubalski, Genetic screen for potassium leaky small mechanosensitive channels (MscS) in *Escherichia coli*: recognition of cytoplasmic beta domain as a new gating element, *J. Biol. Chem.* 286 (2011) 877–888.
- [60] H.R. Malcolm, P. Blount, Mutations in a conserved domain of *E. coli* MscS to the Most conserved superfamily residue leads to kinetic changes, *PLoS One* 10 (2015), e0136756.
- [61] D. Marsh, Electron spin resonance in membrane research: protein–lipid interactions from challenging beginnings to state of the art, *Eur. Biophys. J.* 39 (2010) 513–525.
- [62] T. Nomura, M. Sokabe, K. Yoshimura, Lipid–protein interaction of the MscS mechanosensitive channel examined by scanning mutagenesis, *Biophys. J.* 91 (2006) 2874–2881.
- [63] K. Yoshimura, T. Nomura, M. Sokabe, Loss-of-function mutations at the rim of the funnel of mechanosensitive channel MscL, *Biophys. J.* 86 (2004) 2113–2120.
- [64] R. Phillips, T. Ursell, P. Wiggins, P. Sens, Emerging roles for lipids in shaping membrane–protein function, *Nature*. 459 (2009) 379–385.
- [65] Y.R. Guo, R. MacKinnon, Structure-based membrane dome mechanism for Piezo mechanosensitivity, *Elife*. 6 (2017).
- [66] V. Belyy, A. Anishkin, K. Kamaraju, N. Liu, S. Sukharev, The tension-transmitting ‘clutch’ in the mechanosensitive channel MscS, *Nat. Struct. Mol. Biol.* 17 (2010) 451–458.
- [67] J. Teng, S.H. Loukin, A. Anishkin, C. Kung, A competing hydrophobic tug on L596 to the membrane core unlatches S4–S5 linker elbow from TRP helix and allows TRPV4 channel to open, *Proc. Natl. Acad. Sci. U. S. A.* 113 (2016) 11847–11852.
- [68] J. Teng, S.H. Loukin, A. Anishkin, C. Kung, L596–W733 bond between the start of the S4–S5 linker and the TRP box stabilizes the closed state of TRPV4 channel, *Proc. Natl. Acad. Sci. U. S. A.* 112 (2015) 3386–3391.
- [69] B. Akitake, A. Anishkin, S. Sukharev, The “dashpot” mechanism of stretch-dependent gating in MscS, *J. Gen. Physiol.* 125 (2005) 143–154.
- [70] Y.Y. Dong, A.C. Pike, A. Mackenzie, C. McClenaghan, P. Aryal, L. Dong, et al., K2P channel gating mechanisms revealed by structures of TREK-2 and a complex with Prozac, *Science*. 347 (2015) 1256–1259.
- [71] Carney J, East JM, Mall S, Marius P, Powl AM, Wright JN, et al. Fluorescence quenching methods to study lipid–protein interactions. *Current protocols in protein science/editorial board*, John E Coligan [et al]. 2006;Chapter 19:Unit 19 2.
- [72] S. Miller, M.D. Edwards, C. Ozdemir, I.R. Booth, The closed structure of the MscS mechanosensitive channel—cross-linking of single cysteine mutants, *J. Biol. Chem.* 278 (2003) 32246–32250.
- [73] U. Schumann, M.D. Edwards, T. Rasmussen, W. Bartlett, P. van West, I.R. Booth, YbdG in *Escherichia coli* is a threshold-setting mechanosensitive channel with MscM activity, *Proc. Natl. Acad. Sci. U. S. A.* 107 (2010) 12664–12669.
- [74] T. Rasmussen, M.D. Edwards, S.S. Black, A. Rasmussen, S. Miller, I.R. Booth, Tryptophan in the pore of the mechanosensitive channel MscS: assessment of pore conformations by fluorescence spectroscopy, *J. Biol. Chem.* 285 (2010) 5377–5384.
- [75] A.R. Battle, E. Petrov, P. Pal, B. Martinac, Rapid and improved reconstitution of bacterial mechanosensitive ion channel proteins MscS and MscL into liposomes using a modified sucrose method, *FEBS Lett.* 583 (2009) 407–412.
- [76] P. Blount, S.I. Sukharev, P.C. Moe, B. Martinac, C. Kung, Mechanosensitive channels of bacteria, *Methods Enzymol.* 294 (1999) 458–482.
- [77] J.D. Pilot, J.M. East, A.G. Lee, Effects of bilayer thickness on the activity of diacylglycerol kinase of *Escherichia coli*, *Biochemistry*. 40 (2001) 8188–8195.